Enhancers facilitate the birth of *de novo* genes and their functional integration into regulatory networks

Paco Majic[1,2] & Joshua L. Payne[1,2,*]

1. Institute of Integrative Biology, ETH Zurich, Switzerland

2. Swiss Institute of Bioinformatics, Lausanne, Switzerland

* Correspondence to: joshua.payne@env.ethz.ch

Abstract

Regulatory networks control the spatiotemporal gene expression patterns that give rise to and define the individual cell types of multicellular organisms. In Eumetazoa, distal regulatory elements called enhancers play a key role in determining the structure of such networks, particularly the wiring diagram of "who regulates whom." Mutations that affect enhancer activity can therefore rewire regulatory networks, potentially causing changes in gene expression that may be adaptive. Here, we use single-cell transcriptomic and chromatin accessibility data from mouse to show that enhancers play an additional role in the evolution of regulatory networks: They facilitate network growth by creating transcriptionally active regions of open chromatin that are conducive to *de novo* gene evolution. Specifically, our comparative transcriptomic analysis with three other mammalian species shows that young, mouse-specific transcribed open reading frames are preferentially located near enhancers, whereas older open reading frames are not. Interactions with enhancers are then gained incrementally over macro-evolutionary timescales, helping integrate new genes into existing regulatory networks. Taken together, our results highlight a dual role of enhancers in expanding and rewiring gene regulatory networks.

Introduction

Enhancers are a defining characteristic of eumetazoan gene regulatory networks. They recruit transcription factors and cofactors that "loop out" DNA to bind core promoters and increase the expression of target genes [1, 2], thus mediating interactions between genes. Such interactions are highly dynamic throughout development, facilitating the differential deployment of distinct regulatory sub-networks in different cells, which helps define cell-type specific spatiotemporal gene expression patterns [3, 4].

Enhancer activity is not only dynamic throughout development, but also throughout evolutionary time [5]. The reason is that mutations in enhancer sequences can create or ablate interactions with regulatory proteins, thus enabling modifications in gene use without affecting gene product [6, 7]. Such changes alter a regulatory network's wiring diagram of "who regulates whom," which can cause changes in gene expression patterns that embody or lead to evolutionary adaptations or innovations [8]. Examples include the archetypical pentadactyl limb anatomy of extant tetrapods [9], ocular regression in subterranean rodents [10, 11], limb loss in snakes [11, 12], convergent pigmentation patterns in East African cichlids [13], the mammalian neocortex [14], and cell type diversity in eumetazoans [15].

Regulatory networks not only evolve via rewiring, but also via the addition of new genes [16]. Gene duplication, retrotransposition, gene fusion, the domestication of genomic parasites, and horizontal gene transfer are all means by which new genes can arise from pre-existing genes [17], and thus expand gene regulatory networks. In addition, it is becoming increasingly appreciated that new genes can arise *de novo* from non-coding regions of the genome [18-22]. For protein-coding genes, the essential prerequisites of this process are the formation of an open reading frame (ORF), together with the transcription and translation of that ORF. Because much of the genome is transcribed [23, 24] and many lineage-specific transcripts containing ORFs are potentially translated [25-30], the *de novo* evolution of new protein-coding genes is also a likely contributor to the growth of gene regulatory networks.

An important question concerning *de novo* genes is how they integrate into existing regulatory networks, and what role enhancers may play in this process. It has been hypothesized that enhancer acquisition allows new genes to expand their breadth of expression, providing opportunities to acquire new functions in different cellular contexts [31]. Enhancers may therefore help new genes integrate into existing regulatory networks via edge formation and rewiring. Less appreciated is the role enhancers may

play in the origin of *de novo* genes [32], and thus in the growth of gene regulatory networks. The physical proximity between active enhancers and their target genes [33] – facilitated by DNA looping – creates a transcriptionally permissive environment that is engaged with RNA polymerase II, which may lead to the transcription of regions near the enhancer, or to the transcription of the enhancer itself, producing so-called enhancer RNA [1, 34]. If the resulting transcript is stable, harbors an open reading frame, and engages with ribosomes, then it fulfills the basic prerequisites of *de novo* gene birth. Thus, enhancers may play a dual role in the evolution of *de novo* genes, and consequently in the evolution of gene regulatory networks. By creating a transcriptionally permissive environment that is engaged with the transcriptional machinery, enhancers may facilitate the origin of *de novo* genes; by physically interacting with gene promoters, enhancers may facilitate the integration of *de novo* genes into existing regulatory networks.

Here, we take an integrative approach to study this potential dual role of enhancers. We leverage single-cell transcriptomic and functional genomics data from mouse that describe gene expression levels, chromatin accessibility, and chemical modifications to histones, as well as phylostratigraphic estimates of the ages of transcribed ORFs. We find that the distance between ORFs and enhancers in nucleotide sequence increases with ORF age, indicating that young ORFs preferentially emerge near enhancers. We also find that the number of enhancer interactions per ORF increases with ORF age, even across macro-evolutionary timescales. In sum, our findings support a dual role for enhancers in the origin of *de novo* genes and in their functional integration into gene regulatory networks.

Results

The maturity and age of transcribed open reading frames

To set the stage for our study, we first characterized the maturity and age of a set of mouse transcripts bearing ORFs [29]. Specifically, we characterized the transcript maturity of 46,501 murine ORFs by assessing whether *i*) the ORF resides in a region of open chromatin, which implies it is accessible to the transcriptional machinery; *ii*) the transcript has detectable 5' capping, which confers stability [35, 36], permits its export from the nucleus to the cytoplasm [37] and promotes translation [36]; and *iii*) the transcript associates with ribosomes, indicating the potential for translation [25, 29, 30]. Fig. 1A shows a schematic of our classification of transcript maturity.

We found that over a third (16,735) of the 46,501 ORFs had the highest level of transcript maturity, which we refer to as maturity level 3 (Fig. 1B). The remaining ORFs were distributed among different combinations of the three maturity indicators. We refer to ORFs found in regions of open chromatin as having a maturity level 1 (5,640 ORFs) and those that are also 5' capped as having a maturity level 2 (4,927 ORFs).

The ORFs we assessed had their phylogenetic age estimated by Schmitz et al. [29], based on their presence in the transcriptomes of other mammalian species, including rat, human, and opossum (Fig. 2A). If a homolog of a mouse ORF is found in another species, then it is assumed to have emerged before the common ancestor of that species and mouse. For example, if an ORF is shared with opossum, it is assumed to have originated before the branching of marsupials and placental mammals ~160 million years ago; if it is not shared with any of the other three species, it is assumed to have emerged only after the split between mouse and rat ~20 million years ago. Expectedly, when assessing the distribution of ORFs with each of the maturity indicators across the different age categories, we found that the older an ORF is, the more likely it is to correspond to higher levels of maturity. This is clear from the observation that the percentage of ORFs corresponding to the oldest age class (i.e., opossum) increases with the maturity level, while the percentage corresponding to the youngest age class (i.e., mouse) decreases (Fig. 2B). Furthermore, whereas most mouse-specific ORFs have a maturity level of 1, that fraction gradually decreases as ORFs grow older, while the fraction of ORFs of maturity level 3 increases with age from their minimum in mouse-specific ORFs to their maximum in opossum-shared ORFs (Fig. 2C).

Due to the resolution of the phylogeny shown in Fig. 2A, there is variation in the ages of the ORFs even within a given lineage. We therefore reasoned that such variation might be reflected by variation in transcript maturity. To determine if this was the case, we considered the expression of mouse-specific ORFs from ten different taxa from the mouse branch after the mouse-rat split (Fig. 2D) [23]. Making use of transcriptomic data from those ten taxa, we determined when in the recent phylogenetic history leading to our focal species (*Mus musculus domesticus*) did the genomic regions harboring mouse-specific ORFs start being transcribed. As anticipated, we found that whereas the fraction of non-mouse-specific ORFs with detectable transcription is relatively constant across the different lineages, fewer mouse-specific ORFs are expressed in the lineages that are more distantly related to *M. m. domesticus* (Fig. 2E). We also observed that more mature ORFs are more likely to be transcribed at more basal branches of the mouse

106 phylogeny than are less mature ORFs, indicating that transcript maturity is indicative of when in the mouse
107 phylogeny the genomic region harboring the ORF started being transcribed (Fig. 2F).
108 In sum, these results show that an ORF's transcript maturity increases with its age, complementing
109 previous reports that focused on the correlation between age and translation potential [29]. With these
110 estimates of transcript maturity and age at hand, we next studied the role enhancers play in the birth of *de*
111 *novo* genes and in their integration into regulatory networks.
112
113 *Many young and transcriptionally immature ORFs are proximal to enhancers*
114 H3K27ac and H3K4me1 are histone modifications that are commonly used to identify enhancers,
115 specifically when they are not found overlapping H3K4me3 modifications, which are indicative of
116 promoters [38]. We therefore merged chromatin immunoprecipitation followed by DNA sequencing
117 (ChIP-seq) data for H3K27ac, H3K4me1, and H3K4me3 obtained from 23 mouse tissues and cell types
118 [39], and considered enhancers to be those genomic regions where H3K27ac and/or H3K4me1 peaks do
119 not overlap H3K4me3 peaks in any tissue [40, 41] (Materials and Methods). Assessing the 27,347 ORFs
120 with an assigned maturity level, we found that *i*) mouse-specific ORFs are significantly closer to enhancer
121 marks than ORFs shared with rat, human, or opossum (Spearman's correlation coefficient $\rho = 0.27$, $p <$
122 0.01), with a median distance to their closest enhancer mark of 1,589bp for mouse-specific ORFs
123 compared to more than 2,500bp for the remaining age classes (Fig. 3A); *ii*) over 30% of mouse-specific
124 ORFs are in regions of open chromatin containing enhancer marks, while this percentage decreases as
125 ORFs grow older to less than 5% for those shared with opossum (Fig. 3B); *iii*) significantly more
126 enhancers are found within 50kb upstream and 50kb downstream of mouse-specific ORFs than in any
127 other age class (Fig. S1, Wilcoxon's rank sum test $p < 0.05$); *iv*) the mouse-specific age class has the
128 highest percentage of ORFs showing evidence of bidirectional transcription – a hallmark of enhancer
129 activity [42] (Fig. 3C); and *v*) ORFs of lower transcript maturity, which tend to be younger, are nearer to
130 enhancers than ORFs of higher transcript maturity, which tend to be older (Fig. S2). These results suggest
131 that the birth of many new genes is facilitated by their close proximity to enhancers.
132 Because many (58%) of the mouse-specific ORFs are found in genomic regions that overlap or are
133 very close to genomic regions that harbor annotated genes, we expect that at their birth, such ORFs will
134 inherit the regulatory properties of their host gene, which is older. To specifically assess the regulatory

135 background of ORFs that emerged from or near enhancers and thus did not coopt the regulatory features of
136 the promoters of older genes, we separated ORFs stemming from genomic regions annotated as intergenic
137 (which are the ORFs most likely to have emerged *de novo* [29]) from those that we considered genic,
138 which are those ORFs overlapping other genes or that are near the promoters of other genes (Materials and
139 Methods). We found that intergenic ORFs are considerably more likely to be found closer to enhancers
140 than genic ORFs (Fig. 3D; Fig. S3). For example, ~65% of mouse-specific intergenic ORFs were within
141 1kb of an enhancer, as compared to ~25% for mouse-specific genic ORFs and ~10% for non-mouse-
142 specific ORFs. This implies that ORFs emerging within intergenic regions of the genome lose their
143 proximity to enhancers as they age, perhaps via the transformation of enhancers to promoters [43]. This
144 possibility is supported by the observation that the chromatin modification indicative of promoters,
145 H3K4me3, shows trends opposite to the ones described above for enhancers. That is, older ORFs are
146 closer to a larger number of H3K4me3 marks than younger ORFs (Fig. S4).
147 These observations support the hypothesis that enhancers facilitate the *de novo* evolution of genes
148 from non-coding DNA, and thus contribute to the expansion of gene regulatory networks. However, our
149 analyses so far have considered enhancer marks that were merged across a diversity of cell types and
150 tissues. To provide more direct evidence that enhancers facilitate *de novo* gene birth, we separately
151 considered three tissues (liver, brain, and testis) for which we had both transcriptomic and histone
152 modification data. We found that 24% (100 ORFs), 36% (931 ORFs), and 26% (244 ORFs) of intergenic
153 mouse-specific ORFs with evidence for transcription in liver, brain, and testis, respectively, are within 1kb
154 of an enhancer (Fig. S5). These percentages are considerably lower for genic ORFs (< 8%) and for ORFs
155 shared with rat, human, and opossum (< 2%). Enhancers therefore provide fertile ground for the *de novo*
156 birth of new genes from intergenic regions of the genome.
157
158 *Enhancer interactions are gradually acquired over macro-evolutionary timescales*
159 We next asked how enhancers integrate new genes into existing regulatory networks. The CCCTC-
160 binding factor (CTCF) is an architectural DNA-binding protein that mediates physical interactions between
161 promoters and enhancers [44]. Using ChIP-seq data for CTCF in 15 cell and tissue types, we found that
162 CTCF-bound regions of the genome overlap a larger fraction of older ORFs than younger ORFs (~75% of
163 opossum-shared ORFs compared to ~45% of mouse-specific ORFs; Fig. 4A), that there is a negative

correlation between the age of an ORF and its distance to the closest CTCF-bound region (Spearman's correlation coefficient ρ = -0.27, $p < 0.01$), and that among young mouse-specific ORFs the distance to the closest CTCF peak is significantly higher for intergenic than genic ORFs ($p < 0.01$; Fig. S6). These results suggest that while young ORFs are proximal to enhancers, they are not specifically targeted by them. Such enhancer interactions are likely acquired gradually over time, as CTCF motifs, and other sequence changes conducive to enhancer-promoter interactions, evolve in the proximity of ORFs.

To study how ORFs acquire interactions with enhancers, we considered an enhancer-promoter interaction map derived from single-cell chromatin accessibility data in 13 murine tissues [45] (Materials and Methods). We first corroborated the negative correlation between an ORF's number of enhancer interactions and its distance to the closest CTCF-bound region (Spearman's correlation coefficient ρ = -0.35, $p < 0.01$). We then uncovered a positive correlation between the age of an ORF and its number of enhancer interactions (Spearman's correlation coefficient ρ = 0.17, $p < 0.01$; Fig. 4B). This number increased from a median of 5 enhancer interactions for mouse-specific ORFs to a median of 13 for ORFs that are shared with opossum, indicating that enhancer-promoter interactions are gradually acquired over time. However, when restricting our analysis to ORFs of the highest transcript maturity class, this positive correlation was lost (Spearman's correlation coefficient ρ = 0.001, p = 0.9).

We reasoned that this loss could be because mouse-specific ORFs of genic origin are enriched for transcripts of the highest maturity class (38% as compared to 1.4% for intergenic ORFs). We therefore partitioned the mouse-specific ORFs according to whether they were intergenic or genic, and compared the number of enhancer interactions in these classes to the number of enhancer interactions for non-mouse-specific ORFs. We found that intergenic ORFs had fewer enhancer interactions than genic ORFs, which were similar to non-mouse-specific ORFs in their number of enhancer interactions (Fig. 4C). This suggests that mouse-specific ORFs of genic origin, which are enriched for mature transcripts, tend to coopt the regulatory interactions of their host gene, or of nearby genes. To account for this confounding effect, we considered ORFs that do not share their segment of open chromatin with any other ORF and are therefore unlikely to be coopting the enhancer interactions of other genes (Materials and Methods). We call these 'single ORFs'. We use this distinction, rather than intergenic vs. genic, because only 0.06% of ORFs that emerged before the rat/mouse split are annotated as intergenic, whereas 48% can be considered single ORFs. After making this distinction, we recovered the positive correlation between an ORF's number of

193 enhancer interactions and its age (Spearman's correlation coefficient $\rho = 0.24$, $p < 0.01$); even for ORFs of
194 the highest transcript maturity class, we found that mouse-specific ORFs were involved in fewer
195 interactions than opossum-shared ORFs (Wilcoxon's tailed test, $p < 0.01$; Fig. 4D). Therefore, intergenic
196 mouse-specific ORFs with the highest level of transcript maturity, which tend to be older than those with
197 lower levels of transcript maturity (Fig. 2), have fewer interactions than ORFs in the oldest age class,
198 providing further evidence of the gradual acquisition of enhancer interactions over time.

199 To further explore the pace at which new enhancer interactions are gained over evolutionary time,
200 we shifted our focus to opossum-shared ORFs, most of which (95%) correspond to annotated genes. We
201 separated these into 15 new age classes dating back to the origin of cellular life [46] in order to understand
202 how enhancer interactions are acquired over macroevolutionary timescales (Fig. 5A). With the sole
203 exception of the oldest genes shared with bacteria and archaea, which have significantly fewer interactions
204 than ORFs that emerged before the common ancestor of all eukaryotes, no other age class shows
205 significantly fewer interactions than a younger age class (Fig. 5B; in Fig. S7, note that only a single
206 element below the main diagonal is significant). Disregarding ORFs from the oldest age class, we found a
207 significant correlation between the age of genes and their number of enhancer interactions (Spearman's
208 correlation coefficient $\rho = 0.15$, $p < 0.01$).

209 In sum, young ORFs have relatively few interactions with enhancers, despite being proximal to
210 them in nucleotide sequence. As ORFs age, they gradually acquire enhancer interactions (Fig. 4), a process
211 that continues over macroevolutionary timescales (Fig. 5B).

212

213 *Enhancer acquisition influences expression breadth and variance*

214 We next explored the functional consequences of enhancer acquisition. To do so, we first studied
215 the expression breadth of opossum-shared annotated genes using the phylogeny shown in Fig. 5A and
216 single-cell transcriptomic data from 68 cell types of ten murine tissues [47], for which we also had single-
217 cell chromatin accessibility data (Materials and Methods). We found that expression breadth increases with
218 gene age (Spearman's correlation coefficient $\rho = 0.30$, $p < 0.01$; Fig S8A), corroborating previous analyses
219 performed using transcriptomic data from whole tissues [48]. We additionally found that a gene's
220 expression breadth increases with its number of enhancer interactions (Spearman's correlation coefficient
221 $\rho = 0.37$, $p < 0.01$; Fig. 5C), suggesting that enhancer acquisition has functional consequences.

222 We next measured the coefficient of variation for the expression of each gene, a measure that is
223 useful for identifying stably vs. variably expressed genes from single cell RNA sequencing [49]. It is
224 calculated as the standard deviation of a gene's expression across cell types, divided by the mean
225 expression across cell types (Materials and Methods). Genes with a lower coefficient of variation tend to
226 be more tightly regulated than those with a higher coefficient of variation [49]. We found a significant
227 correlation between the coefficient of variation and gene age (Spearman's correlation coefficient ρ = -0.32,
228 $p < 0.01$; Fig. S8B), as well as with a gene's number of enhancer interactions (Spearman's correlation
229 coefficient ρ = -0.32, $p < 0.01$; Fig 5D). Specifically, the coefficient of variation decreases as genes acquire
230 more enhancer interactions, stabilizing around one when genes acquire at least 20 enhancer interactions.
231 These results show that enhancer acquisition affects gene expression breadth and variance, further
232 supporting the role of enhancers in the integration of genes into regulatory networks.
233
234 **Discussion**

235 We report a dual role of enhancers in the evolution of gene regulatory networks: They engage with
236 the transcriptional machinery to create an environment of open chromatin that is conducive to the *de novo*
237 birth of new genes, and they help integrate these new genes into existing regulatory networks by
238 interacting with gene promoters, thus facilitating the evolution of controlled and robust gene expression in
239 space and time.

240 Our study provides empirical support for the hypothesis that enhancers may facilitate *de novo* gene
241 evolution, which to our knowledge was first proposed upon the discovery of enhancer RNA [34] and later
242 expanded upon in a perspective piece by Wu and Sharp [32]. Our findings complement contemporaneous
243 work [50] on the regulatory architecture of the nematode *Pristionchus pacificus*, which showed that young
244 genes – those private to *P. pacificus* – are in closer proximity to enhancers than genes with one-to-one
245 orthologs in other nematode species. The observation that enhancers facilitate *de novo* gene birth in both
246 nematodes and mammals suggests that this mode of *de novo* gene evolution dates back to at least the
247 common ancestor of Bilateria, and possibly even earlier, since cnidarians and ctenophores also employ
248 distal regulatory elements [15, 51, 52].

The facilitating role of enhancers in *de novo* gene birth is conceptually similar to the facilitating role of the permissive chromatin state of meiotic spermatocytes and post-meiotic round spermatids that underlies the "out-of-testis hypothesis," which proposes the testis as a primary tissue for the origination of new genes [17]. Both scenarios envision regions of open chromatin that are exposed to the transcriptional machinery, and thus produce a transcriptionally active environment that is conducive to the evolution of new genes. The two scenarios differ, however, in at least two ways. First, genes that emerge from or near enhancers may rapidly acquire their own promoters, due to the similar architectural and functional features of enhancers and promoters, a similarity that facilitates the rapid turnover of the former to the latter [43]. Second, enhancers are often deployed in multiple cell types or developmental stages [53], exposing enhancer-proximal *de novo* genes to distinct cellular contexts where they may confer a selective advantage.

The hypothesis that enhancers help *de novo* genes integrate into existing regulatory networks was previously proposed in the context of the out-of-testis hypothesis, as a means to expand a new gene's breadth of expression [31]. Using single-cell chromatin accessibility and transcriptomic data, our study provides the first empirical support for the hypothesis that *de novo* genes gradually acquire enhancer interactions over time, and that this acquisition increases expression breadth. These findings complement related studies of gene integration into cellular networks, such as networks of protein-protein interactions [54, 55]. Our observation that genes continue to acquire enhancer interactions over macro-evolutionary timescales mirrors similar increases in other aspects of gene regulation, such as in the number of proximal transcription factor binding sites, alternative transcript isoforms, and miRNA targets [56].

Regulatory networks drive the spatiotemporal gene expression patterns that give rise to and define the numerous and distinct cellular identities characteristic of Metazoan life. Enhancers play an integral role in this process, mediating cell-type-specific gene-gene interactions, thus facilitating the combinatorial deployment of different genes in different contexts. Genetic changes that affect such interactions are responsible for myriad evolutionary adaptations and innovations [6-8, 57]. Our results suggest that the power of enhancers in creating such evolutionary novelties lies not only in their ability to rewire gene regulatory networks, but also in their ability to expand them, by providing fertile ground for *de novo* gene birth.

Materials and methods

ORF age and transcript maturity

Schmitz et al. [29] identified a set of 58,864 ORFs from the transcriptomes of three murine tissues: liver, testis, and brain. Blasting against the transcriptomes of four other mammalian species (rat, human, kangaroo rat, and opossum), they estimated the age of each ORF by phylostratigraphic methods [29, 58]. Because of the small number of ORFs shared with the kangaroo rat (49 ORFs), we merged these ORFs together with those from the rat age class. We used the genomic coordinates of the first exon of each ORF in the mm10 mouse genome reference to study the regulatory properties of ORFs of different ages, for example to study their distance to the nearest enhancer.

We considered three indicators of ORF transcript maturity:

i) Open chromatin: We used single-cell ATAC-seq data from 13 different mouse tissues (bone marrow, cerebellum, large intestine, heart, small intestine, kidney, liver, lung, cortex, spleen, testes, thymus, and whole brain). The ATAC-seq method detects regions of open chromatin through the insertion of transposons in random accessible regions of the genome that can later be sequenced [59]. We obtained the data from the Mouse ATAC atlas [45], which comprised 436,206 peaks of open chromatin. We used liftOver from the Genome Browser at UCSC [60] to convert the genome coordinates from mm9 to mm10. A total of 29 peaks could not be converted. Using the "intersect" function of bedtools with default parameters [61], we found which ORFs have their first exons in regions of open chromatin and are therefore accessible to the transcriptional machinery in at least one of the tissues.

ii) 5' capping: We used cap analysis of gene expression (CAGE) data from the FANTOM5 consortium from 1,016 mouse samples including cell lines, primary cells and tissues [62, 63]. This method is based on the capture of 5' capped ends of mRNA, which allows the mapping of regions of transcription initiation genome-wide [64]. Using the "closest" function from bedtools with default parameters [61], we measured the distance between an ORF's first exon and its closest CAGE peak. We considered a transcript to be 5' capped if the start site of its first exon was located within 200 bases of a CAGE peak (Fig. S9).

305 *iii) Ribosome association:* We used ribosome profiling (ribo-seq) data from 9 different mouse
306 tissues (embryonic stem cells, neutrophils, fibroblasts, liver, brain, testis, epidermis, kidney, and
307 adipose tissue). This method is based on the sequencing of mRNA fragments that are protected from
308 RNase digestion by ribosomes [65]. We obtained the coordinates of mRNA segments detected by ribo-
309 seq from GWIPS-viz [66], a database that includes such data from different studies. Following Schmitz
310 et al. [29], we considered an ORF as being potentially translated if at least one read from the ribo-seq
311 datasets could be assigned to the ORF in question.

312 Using these indicators, we defined three levels of transcript maturity: maturity level 1 for ORFs
313 whose first exon overlaps open chromatin, maturity level 2 for ORFs that are also 5' capped, and maturity
314 level 3 for ORFs that also associate to ribosomes. Because the ribo-seq data may be limited by the
315 detectability of the transcript [29], we only considered ORFs that were also found in the mRNA-seq
316 dataset available at GWIPS-viz; this filter lead us to only consider a subset of the ORFs reported by
317 Schmitz et al. [29]. Specifically, we assigned transcript maturity levels to 46,501 ORFs (~79% of the
318 58,864 ORFs).

319 To determine if transcript maturity correlates with gene age even within the mouse lineage, we
320 considered the transcriptomes of brain, liver and testis from 10 different mouse taxa (3 populations of *Mus*
321 *musculus domesticus*, 2 populations of *M. m. musculus*, and 1 from *M. m. castaneus*, *M. spicilegus*, *M.*
322 *spretus*, *M. mattheyi* and *Apodemus uralensis*). The data consisted of read counts from the transcriptomes
323 of each taxon mapped to 200 bp windows of the mm10 mouse reference genome [23]. We considered an
324 ORF to be expressed in any of the ten taxa if at least 10 reads (the upper threshold to be considered "lowly
325 expressed" [23]) could be detected in the 200 bp windows overlapping at least 60% of the length of the
326 first exon of the ORF.

327

328 *Enhancer association*

329 We obtained ChIP-seq data for H3K27ac, H3K4me1, and H3K4me3 modifications from 23
330 different tissues and cell types from the ENCODE project (bone marrow, cerebellum, cortex, heart, kidney,
331 liver, lung, olfactory bulb, placenta, spleen, small intestine, testis, thymus, embryonic whole brain,
332 embryonic liver, embryonic limb, brown adipose tissue, macrophages, MEL, MEF, mESC, CH12 cell line,
333 and E14 embryonic mouse) [39]. We used liftover to convert the genomic coordinates of the peaks from

334 mm9 to mm10. We used the "merge" function of bedtools with default parameters to collate the peaks for
335 all tissues and cell types, considering any overlapping H3K27ac and H3K4me1 peak as part of the same
336 enhancer. We used the "intersect" function of bedtools with default parameters to separate H3K27ac and
337 H3K4me1 peaks that overlapped any length of H3K4me3 peaks from those that did not. This resulted in
338 172,930 H3K27ac and 277,187 H3K4me1 peaks that did not overlap H3K4me3 peaks. We considered
339 genomic regions with H3K4me3 peaks to be promoters, and those exclusively with H3K27ac and/or
340 H3K4me1 peaks to be enhancers [41]. We measured the distance in base pairs between the first exon of an
341 ORF to an enhancer or promoter using the "closest" function of bedtools with default parameters. To
342 assess the number of enhancers surrounding an ORF, we considered the 50,000 base pairs upstream and
343 downstream of the first exon of each ORF, and determined the number of H3K27ac and H3K4me1 peaks
344 within that window.

345 We also studied the association of ORFs that are expressed in different tissues to chromatin
346 modifications in those same tissues. To do so, we used the transcriptomic data for brain, testis and liver
347 from the samples of *Mus musculus domesticus* as described in the previous section to classify ORFs as
348 expressed or not expressed in each tissue. We determined the fraction of ORFs expressed in each tissue
349 that were up to 1kb away from a H3K4me1, H3K27ac and H3K4me3 ChIP-seq peak identified from liver,
350 testis, embryonic whole brain, and cortex samples.

351 We also considered bidirectional CAGE peaks, which are indicative of enhancers [42, 67]. We
352 assigned bidirectional CAGE peaks to ORFs using the same criteria we used to assign H3K27ac and
353 H3K4me1 peaks to ORFs, as described above.

354

355 *ORF origin*

356 Schmitz et al. [29] annotated each ORF as belonging to one of 8 different categories: "intergenic,"
357 "close to promoter same strand," "close to promoter opposite strand," "overlapping same strand,"
358 "overlapping opposite strand," "overlapping coding sequence same strand," "overlapping coding sequence
359 opposite strand," and "overlapping annotated gene in frame." We considered all categories except
360 "intergenic" to be "genic" in order to separate ORFs that are born within or near existing genes from those
361 that are not. This classification is more challenging for non-mouse-specific ORFs due to the better
362 annotation of older genes [29], which makes them more likely to correspond to the "overlapping annotated

363 gene in frame" category even if they are of intergenic origin. We therefore further classified ORFs
364 according to whether they shared their segment of open chromatin with another ORF. Specifically, we
365 classified an ORF as "shared" if its first exon was in the same segment of open chromatin as the first exon
366 of any other ORF, and as "single" otherwise.
367
368 *Enhancer interactions*
369 As with H3K27ac, H3K4me1, and H3K4me3 histone modifications, we evaluated the distance of
370 each ORF to CTCF ChIP-seq peaks obtained from 15 different cell and tissue types (bone marrow,
371 cerebellum, cortex, heart, kidney, developing limb during stage E14.5, liver, fibroblasts, mESC, olfactory
372 bulb, small intestine, spleen, testis, thymus and the whole brain) [39]. We used liftOver to convert the data
373 from mm9 to mm10.
374 Cusanovich et al. [45] used single-cell ATAC-seq data to predict physical interactions between
375 regions of open chromatin [68], thus creating an atlas of enhancer interactions in single murine cells. We
376 downloaded these data from the Mouse ATAC atlas [45], which includes the cell clusters where the
377 interactions occur, as well as the co-accessibility scores of pairs of regions of open chromatin – a measure
378 of interaction strength. We disregarded cell clusters classified as "unknown" or "collisions", as well as
379 interactions with a co-accessibility score lower than 0.25, following Pliner et al. [68]. We also filtered out
380 interactions with regions of open chromatin that harbored annotated promoters, in order to focus solely on
381 interactions with enhancers. An interaction was assigned to an ORF if the ORF's first exon was included in
382 the interaction.
383
384 *Age of annotated genes*
385 To study how genes acquire enhancer interactions over macro-evolutionary timescales, we
386 considered the subset of ORFs that belong to the opossum age class in Schmitz et al. [29] and that are
387 annotated as genes in the latest version of Ensembl (release 95) [69]. We matched these genes to age
388 estimates reported by Neme & Tautz [46], based on a phylostratigraphic analysis of 20 lineages spanning 4
389 billion years from the last universal common ancestor to the common ancestor of mouse and rat. We
390 further filtered the dataset to only include ORFs that emerged in the first 15 of the 20 phylostrata, in order
391 to focus on ORFs that are considered to have emerged before the split between the common ancestor of

392 placental mammals and marsupials by both Schmitz et al. [29] and Neme & Tautz [46]. This left us with
393 ~16,000 ORFs corresponding to annotated genes that emerged prior to the origin of placental mammals.
394
395 *Breadth of expression*
396 To study the transcription of annotated genes, we used the expression data reported by the Tabula
397 Muris Consortium [47] for the single-cell RNA sequencing performed with FACS-based cell capture in
398 plates, for 20 different mouse tissues. The data include the log-normalization of 1 + counts per million for
399 each of the annotated genes in each of the sequenced cells. We considered ten tissues that were also used
400 for the construction of the Mouse ATAC Atlas [45]. We measured the expression breadth of each ORF
401 corresponding to an annotated gene as the number of cell types in which expression could be detected in at
402 least 5% of the cells assigned to a cell type. Additionally, we calculated the coefficient of variation of the
403 expression of each gene as the standard deviation over the mean of the log-normalisation of 1 + counts per
404 million across cell types.
405

406 **Figures**
407
408

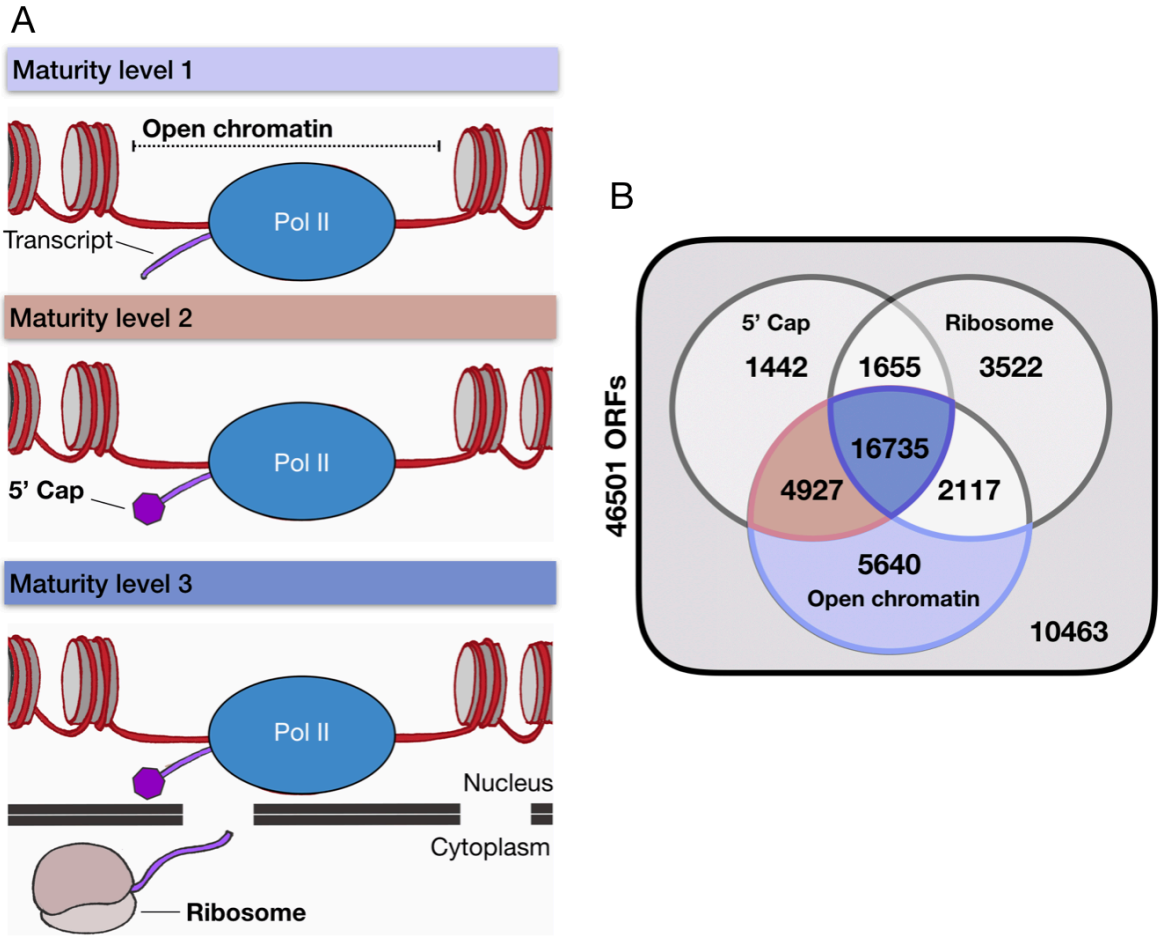

409
410
411 Figure 1. Three levels of transcript maturity. A) Maturity level 1 refers to ORFs that are in regions of open
412 chromatin, but have none of the other maturity indicators; ORFs of maturity level 2 are in regions of open
413 chromatin and are 5' capped, but have no evidence of association with ribosomes; ORFs of maturity level
414 3 are in regions of open chromatin, are 5' capped, and show evidence of association with ribosomes. B)
415 Venn diagram of the number of ORFs associated with each maturity indicator. Colors correspond to the
416 pallet used in A.
417
418

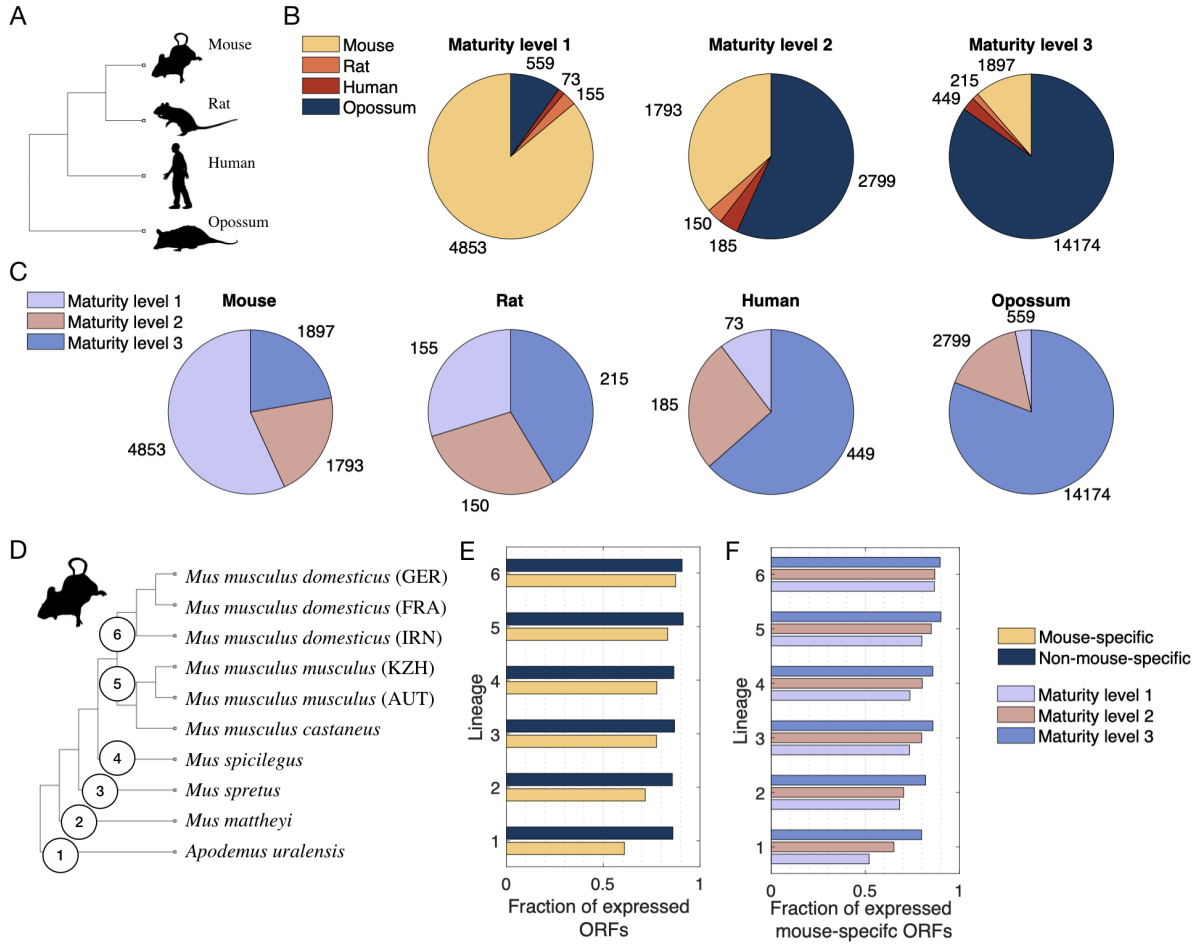

Figure 2. Transcript maturity level and ORF age. A) Phylogenetic relationship between mouse, rat, human, and opossum – the four species defining each age class. B) Pie charts of the distribution of ORFs from each maturity level among the different age classes. C) Pie charts of the distribution of ORFs from each age class among the different maturity levels. D) Phylogeny adapted from Neme & Tautz [23] of ten mouse taxa used to study the association between the transcription and the maturity level of mouse-specific ORFs. The numbered circles indicate the mouse lineages used for transcriptomic comparisons. E) Fraction of mouse-specific and non-mouse-specific ORFs for which there is evidence of transcription in brain, testis and/or liver in at least one of the taxa included in each of the six mouse lineages. F) Fraction of mouse-specific ORFs of each maturity level with detectable transcription in at least one of the taxa included in each of the six mouse lineages.

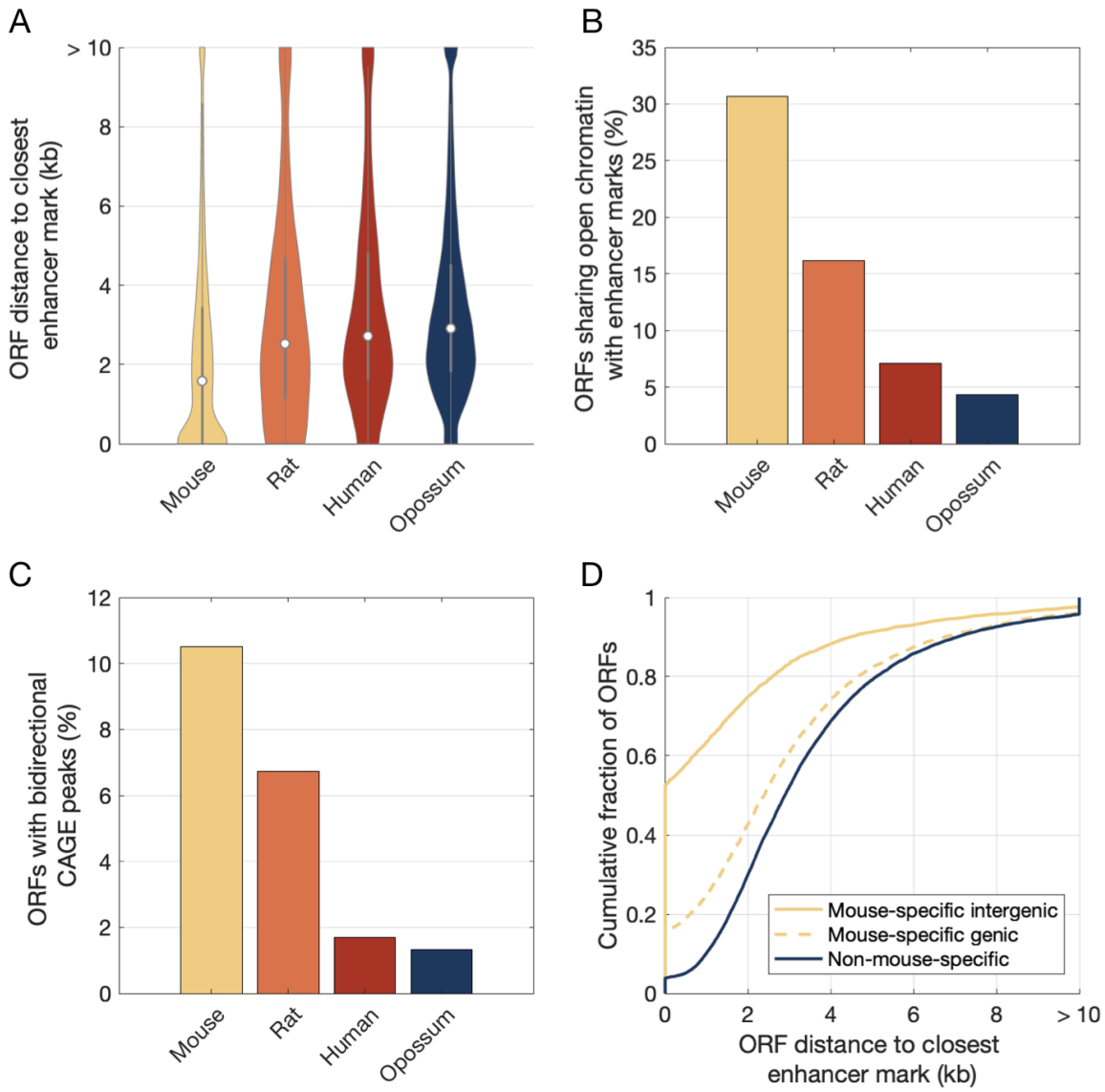

Figure 3. Enhancers facilitate *de novo* gene birth. A) Distance between each ORF and its closest H3K27ac and/or H3K4me1 peak, as a function of ORF age. B) Fraction of ORFs of each age class that share their segment of open chromatin with an enhancer mark. C) Fraction of ORFs from each age class that are within 200bp of a CAGE peak that is annotated as bidirectional [67]. D) Cumulative fraction of mouse-specific ORFs from genic and intergenic regions, as well as non-mouse-specific ORFs, as a function of their proximity to enhancer marks.

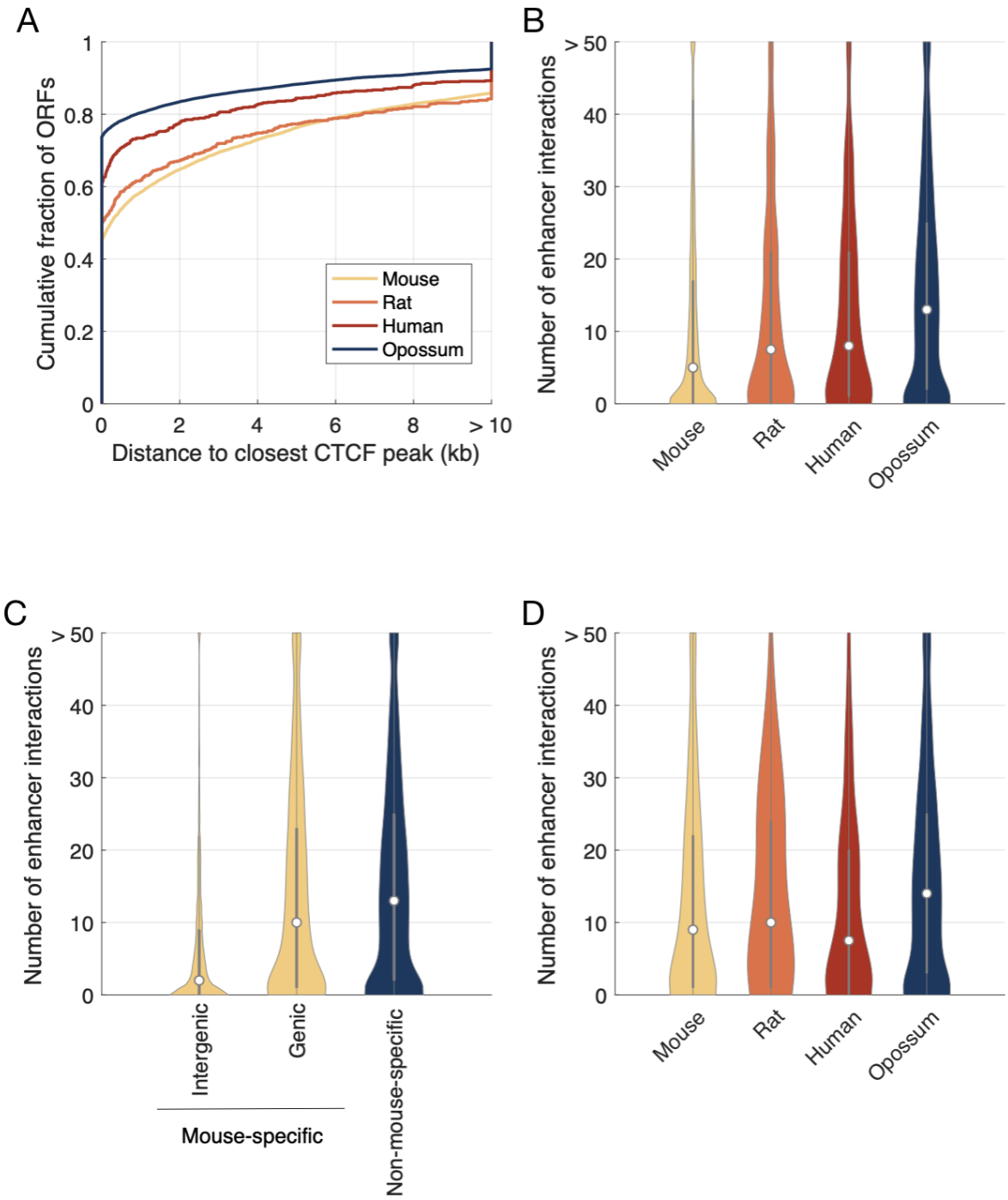

Figure 4. The number of enhancer interactions increases with ORF age. A) Cumulative fraction of ORFs of each age class as a function of their distance to the closest CTCF peak. B) Number of enhancer interactions of ORFs from each age class. C) Number of enhancer interactions of non-mouse-specific, mouse-specific genic, and mouse-specific intergenic ORFs. D) Number of interactions of single ORFs of maturity level 3 from each age class.

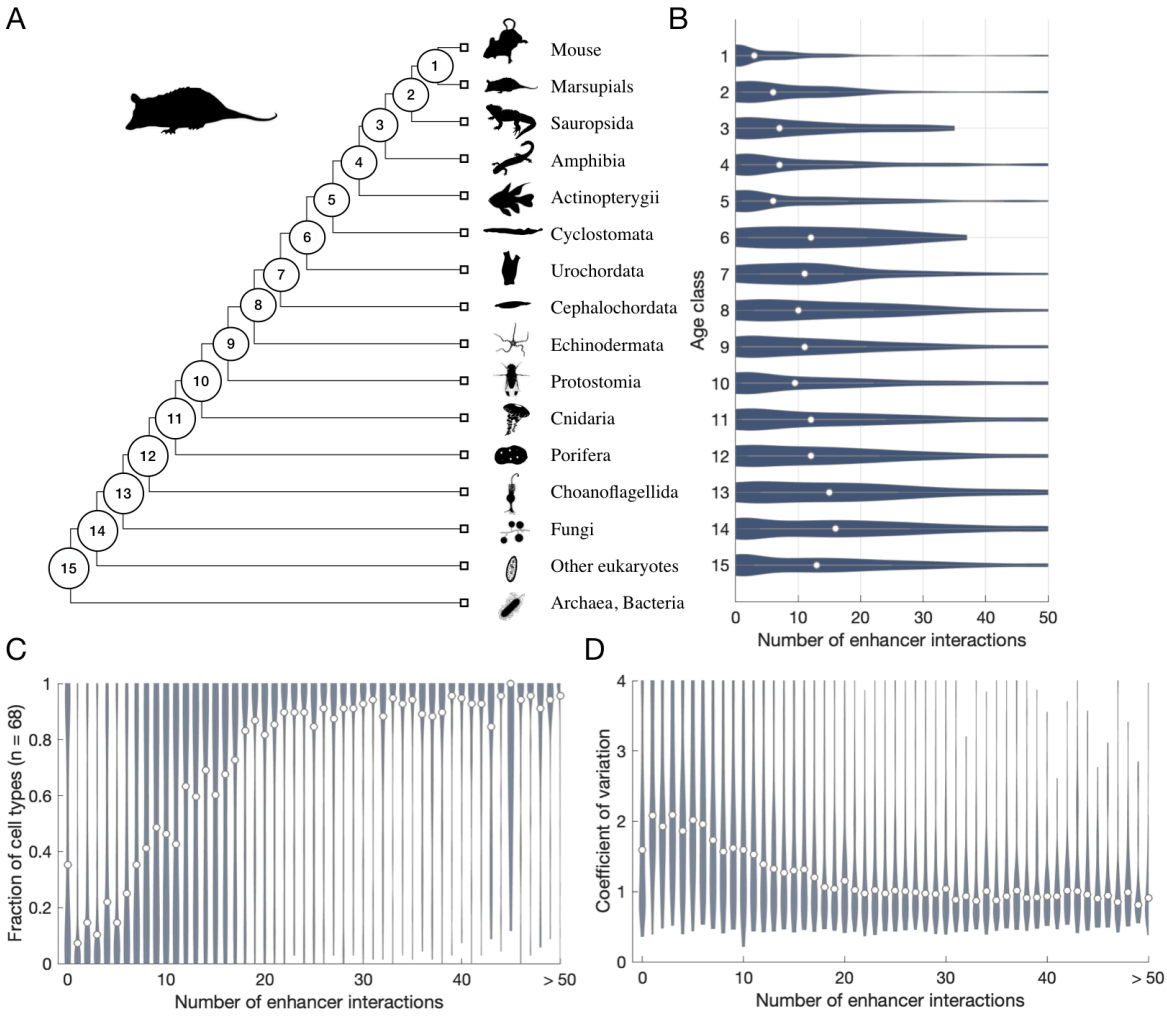

Figure 5. Enhancers facilitate the functional integration of genes into regulatory networks across macroevolutionary timescales. A) Phylogeny adapted from [46]. The numbered circles indicate lineages representative of the age classes to which genes were assigned. B) Number of enhancer interactions per gene as a function of gene age. C) Expression breadth and D) coefficient of variation as a function of the number of enhancer interactions.

459 **Supplementary figures**
460

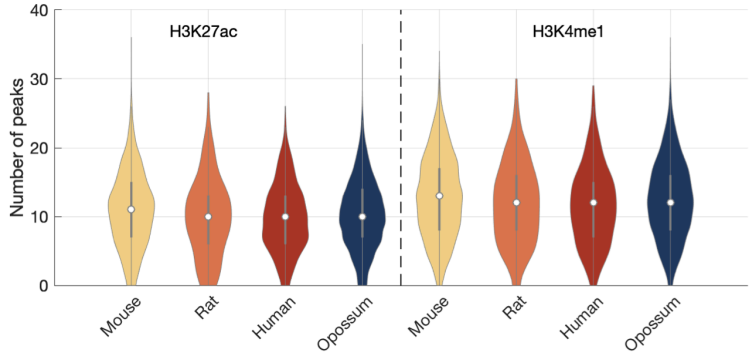

461
462 Figure S1. More enhancers are found near mouse-specific ORFs than are found near older ORFs. The
463 number of H3K27ac and H3K4me1 peaks flanking ORFs within 50kb upstream and 50kb downstream is
464 shown as a function of ORF age.
465
466
467

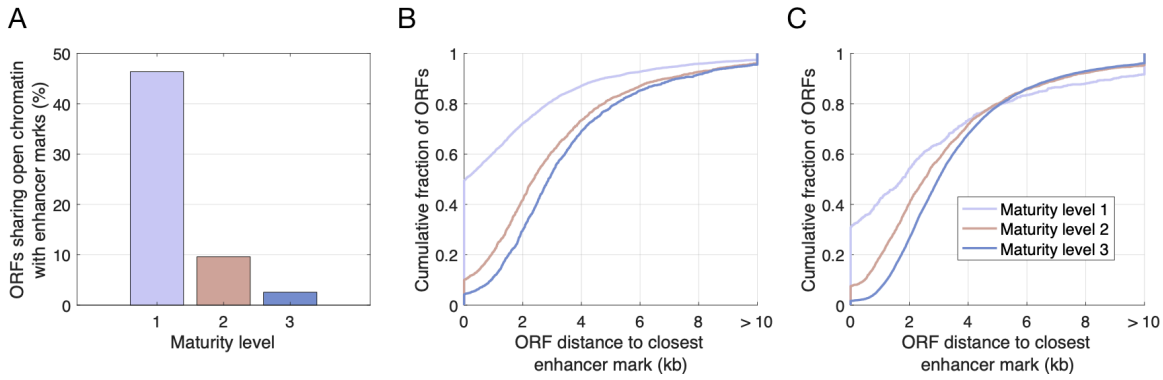

468
469 Figure S2. Distance to enhancers increases with transcript maturity. A) Fraction of ORFs of each maturity
470 level that share their segment of open chromatin with an H3K27ac and/or H3K4me1 peak. Cumulative
471 fraction of B) mouse-specific and C) non-mouse specific ORFs classified according to their maturity level,
472 as a function of their proximity to the closest enhancer mark.
473

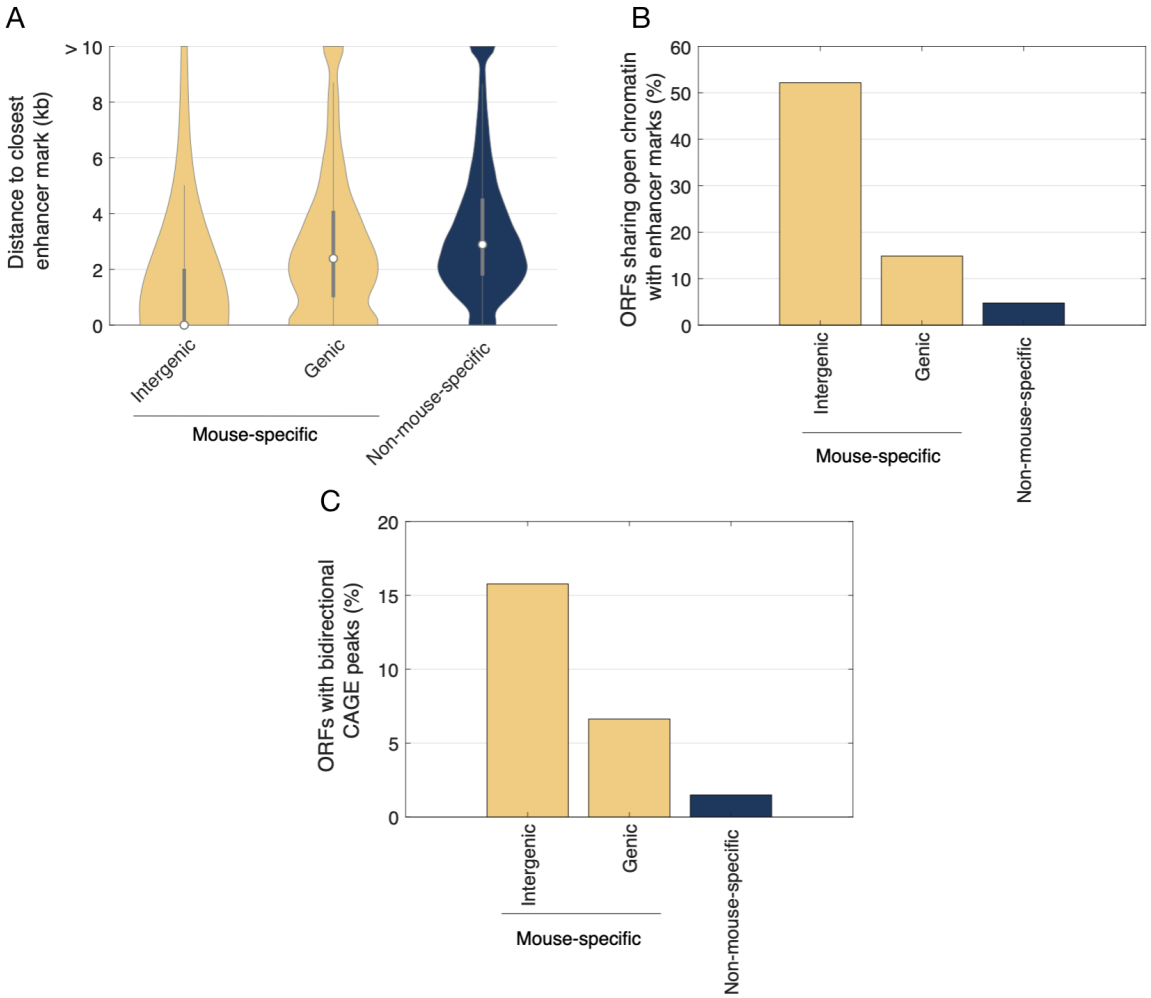

Figure S3. Mouse-specific ORFs transcribed from intergenic regions are close to enhancers. A) Distance between each ORF and its closest H3K27ac and/or H3K4me1 peak, as a function of the genomic annotation of each ORF. B) Fraction of intergenic, genic and non-mouse-specific ORFs that share their segment of open chromatin with an enhancer mark. C) Fraction of intergenic, genic and non-mouse-specific ORFs that are within 200bp of a CAGE peak that is annotated as bidirectional [67].

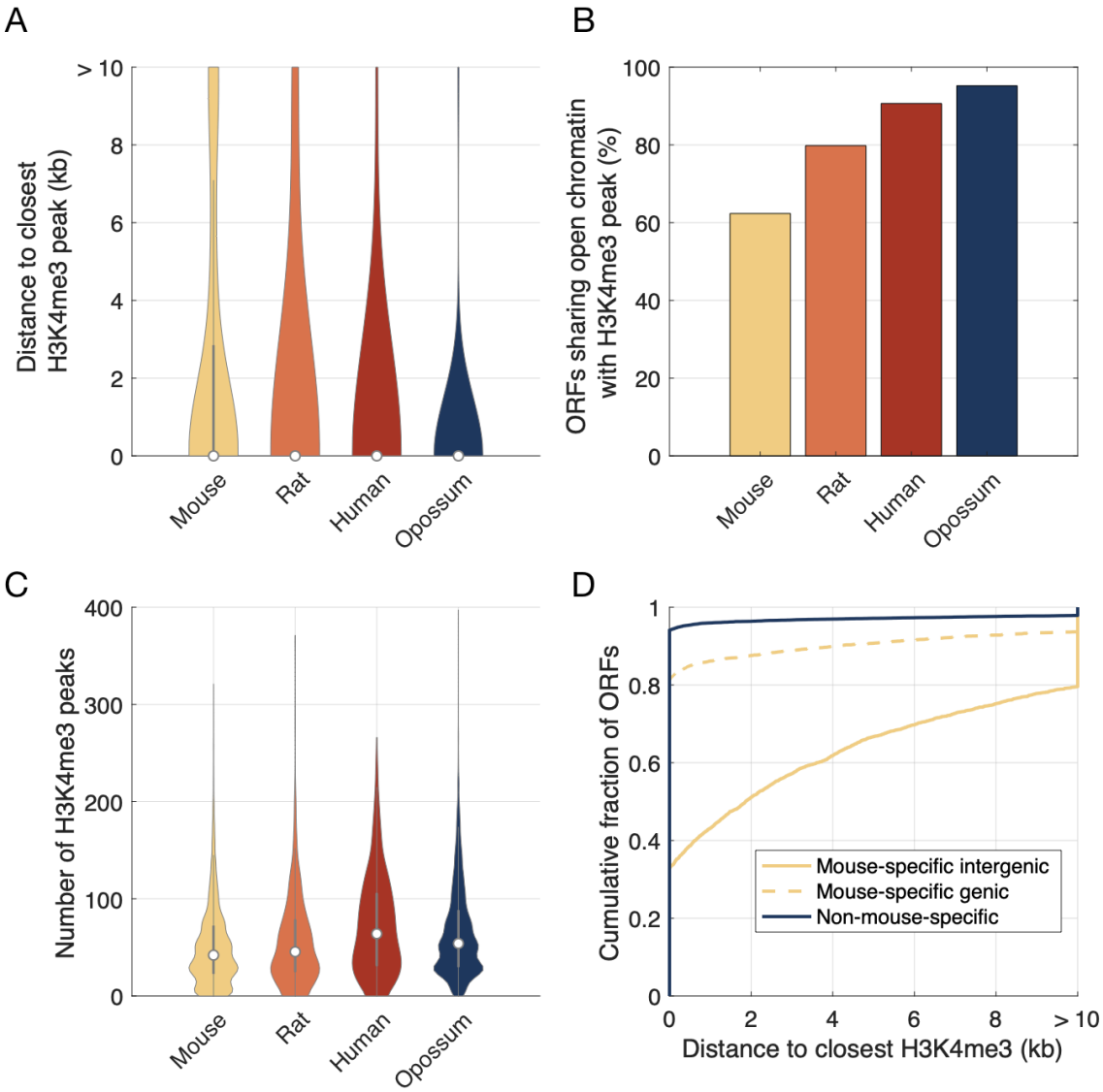

Figure S4. Older ORFs are nearer to promoters than younger ORFs. A) Distance between each ORF and its closest H3K4me3 peak, as a function of ORF age. B) Fraction of ORFs of each age class that share their segment of open chromatin with an H3K4me3 mark. C) Number of H3K4me3 peaks within 50 kb upstream or downstream of an ORF, as a function of ORF age. D) Cumulative fraction of mouse-specific ORFs from genic (dashed yellow line) and intergenic (solid yellow line) genomic regions, as well as non-mouse-specific ORFs (blue line), as a function of their proximity to H3K4me3 peaks.

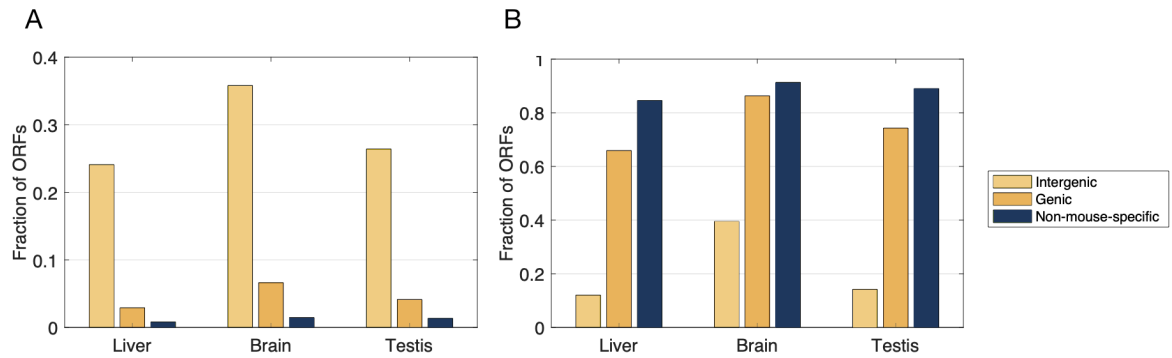

Figure S5. Intergenic ORFs preferentially emerge near enhancers. Fraction of ORFs expressed in liver, brain, and testis that are within 1kb of an active A) enhancer mark (i.e., H3K27ac or H3K4me1) or B) promoter mark (i.e., H3K4me3) in each tissue.

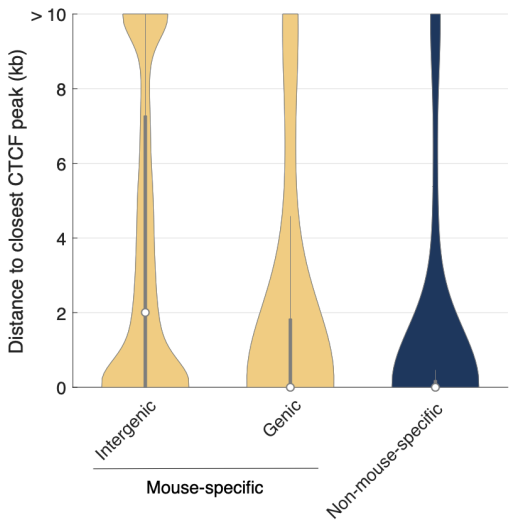

Figure S6. Intergenic ORFs are farther away from CTCF-bound regions. Distance between each ORF and its closest CTCF peak for intergenic, genic and non-mouse-specific ORFs.

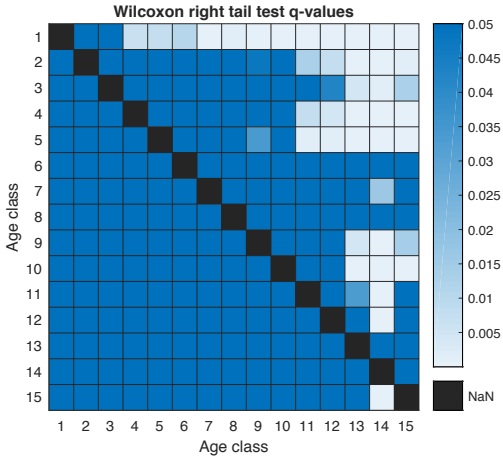

Figure S7. Heatmap of FDR-corrected q-values for the Wilcoxon right-tailed test between the number of distal interactions from each pair of age classes. Darker colors indicate higher q-values. All comparisons with a value greater than or equal to 0.05 are the darkest shade and are considered non-significant.

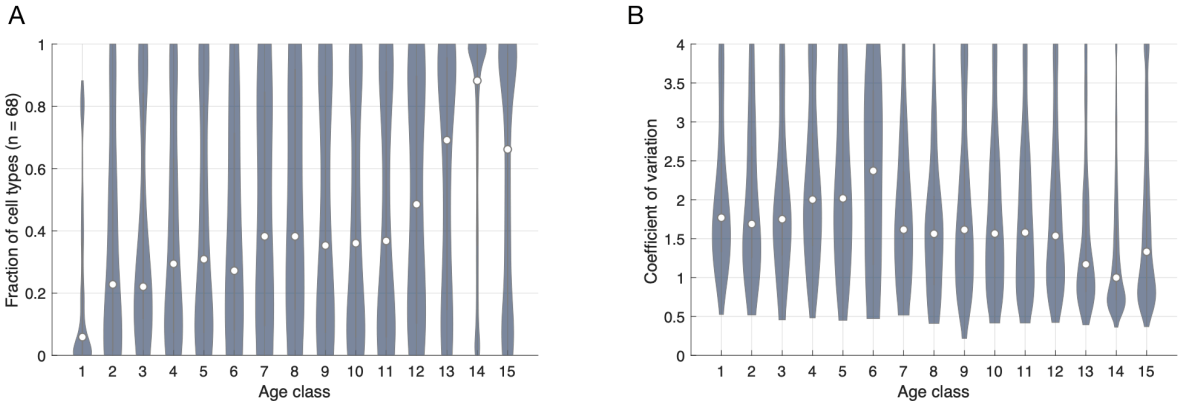

Figure S8. Expression breadth and variance correlate with gene age. A) Fraction of cell types in which there is detectable expression of annotated genes (in at least 5% of the cells included in the cell type cluster) as a function of gene age. B) Coefficient of variation of annotated genes as a function of gene age.

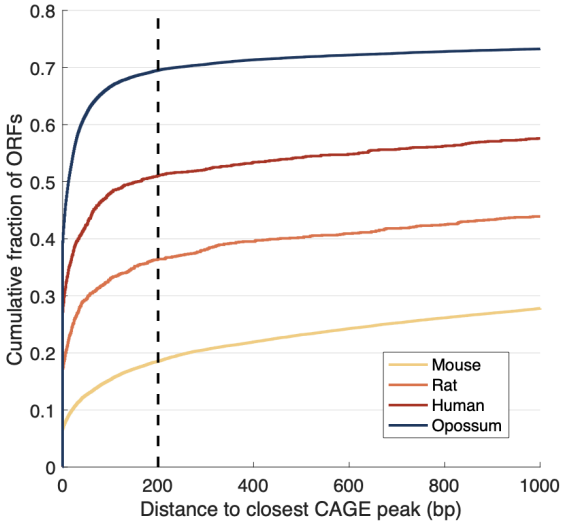

Figure S9. Cumulative fraction of ORFs of each age class as a function of the distance to the closest CAGE peak. The vertical dashed line indicates the threshold we used to consider an ORF as 5' capped because of its proximity to a CAGE peak.

528 **References**

529 1. Haberle V, Stark A. Eukaryotic core promoters and the functional basis of
530 transcription initiation. Nat Rev Mol Cell Biol. 2018;19(10):621-37. Epub 2018/06/28. doi:
531 10.1038/s41580-018-0028-8. PubMed PMID: 29946135; PubMed Central PMCID:
532 PMCPMC6205604.
533 2. Catarino RR, Stark A. Assessing sufficiency and necessity of enhancer activities for
534 gene expression and the mechanisms of transcription activation. Genes & Development.
535 2018;32(3-4):202-23. doi: 10.1101/gad.310367.117.
536 3. Davidson EH, Levine MS. Properties of developmental gene regulatory networks.
537 Proc Natl Acad Sci U S A. 2008;105(51):20063-6. Epub 2008/12/24. doi:
538 10.1073/pnas.0806007105. PubMed PMID: 19104053; PubMed Central PMCID:
539 PMCPMC2629280.
540 4. Spitz F, Furlong EEM. Transcription factors: from enhancer binding to developmental
541 control. Nat Rev Genet. 2012;13(9):613-26. doi: 10.1038/nrg3207.
542 5. Villar D, Berthelot C, Aldridge S, Rayner Tim F, Lukk M, Pignatelli M, et al.
543 Enhancer Evolution across 20 Mammalian Species. Cell. 2015;160(3):554-66. doi:
544 10.1016/j.cell.2015.01.006.
545 6. Prud'homme B, Gompel N, Carroll SB. Emerging principles of regulatory evolution.
546 Proceedings of the National Academy of Sciences. 2007;104(Supplement 1):8605-12. doi:
547 10.1073/pnas.0700488104.
548 7. Carroll SB. Evo-Devo and an Expanding Evolutionary Synthesis: A Genetic Theory
549 of Morphological Evolution. Cell. 2008;134(1):25-36. doi: 10.1016/j.cell.2008.06.030.
550 8. Peter Isabelle S, Davidson Eric H. Evolution of Gene Regulatory Networks
551 Controlling Body Plan Development. Cell. 2011;144(6):970-85. doi:
552 10.1016/j.cell.2011.02.017.
553 9. Kherdjemil Y, Lalonde RL, Sheth R, Dumouchel A, de Martino G, Pineault KM, et
554 al. Evolution of Hoxa11 regulation in vertebrates is linked to the pentadactyl state. Nature.
555 2016;539(7627):89-92. doi: 10.1038/nature19813.
556 10. Partha R, Chauhan BK, Ferreira Z, Robinson JD, Lathrop K, Nischal KK, et al.
557 Subterranean mammals show convergent regression in ocular genes and enhancers, along
558 with adaptation to tunneling. eLife. 2017;6. doi: 10.7554/eLife.25884.
559 11. Roscito JG, Sameith K, Parra G, Langer BE, Petzold A, Moebius C, et al. Phenotype
560 loss is associated with widespread divergence of the gene regulatory landscape in evolution.
561 Nature Communications. 2018;9(1). doi: 10.1038/s41467-018-07122-z.
562 12. Kvon EZ, Kamneva OK, Melo US, Barozzi I, Osterwalder M, Mannion BJ, et al.
563 Progressive Loss of Function in a Limb Enhancer during Snake Evolution. Cell.
564 2016;167(3):633-42.e11. doi: 10.1016/j.cell.2016.09.028.
565 13. Kratochwil CF, Liang Y, Gerwin J, Woltering JM, Urban S, Henning F, et al. Agouti-
566 related peptide 2 facilitates convergent evolution of stripe patterns across cichlid fish
567 radiations. Science. 2018;362(6413):457-60. doi: 10.1126/science.aao6809.
568 14. Emera D, Yin J, Reilly SK, Gockley J, Noonan JP. Origin and evolution of
569 developmental enhancers in the mammalian neocortex. Proc Natl Acad Sci U S A.
570 2016;113(19):E2617-26. Epub 2016/04/27. doi: 10.1073/pnas.1603718113. PubMed PMID:
571 27114548; PubMed Central PMCID: PMCPMC4868431.
572 15. Sebe-Pedros A, Chomsky E, Pang K, Lara-Astiaso D, Gaiti F, Mukamel Z, et al.
573 Early metazoan cell type diversity and the evolution of multicellular gene regulation. Nat
574 Ecol Evol. 2018;2(7):1176-88. Epub 2018/06/27. doi: 10.1038/s41559-018-0575-6. PubMed
575 PMID: 29942020; PubMed Central PMCID: PMCPMC6040636.

576 16. Teichmann SA, Babu MM. Gene regulatory network growth by duplication. Nature
577 Genetics. 2004;36(5):492-6. doi: 10.1038/ng1340.
578 17. Kaessmann H. Origins, evolution, and phenotypic impact of new genes. Genome Res.
579 2010;20(10):1313-26. Epub 2010/07/24. doi: 10.1101/gr.101386.109. PubMed PMID:
580 20651121; PubMed Central PMCID: PMCPMC2945180.
581 18. McLysaght A, Hurst LD. Open questions in the study of de novo genes: what, how
582 and why. Nat Rev Genet. 2016;17(9):567-78. doi: 10.1038/nrg.2016.78. PubMed PMID:
583 WOS:000381510700013.
584 19. Xie C, Bekpen C, Künzel S, Keshavarz M, Krebs-Wheaton R, Skrabar N, et al. 2019.
585 doi: 10.1101/510214.
586 20. Betran E, Reinhardt JA, Wanjiru BM, Brant AT, Saelao P, Begun DJ, et al. De Novo
587 ORFs in Drosophila Are Important to Organismal Fitness and Evolved Rapidly from
588 Previously Non-coding Sequences. PLoS Genetics. 2013;9(10). doi:
589 10.1371/journal.pgen.1003860.
590 21. Kim SK, Mayer MG, Rödelsperger C, Witte H, Riebesell M, Sommer RJ. The Orphan
591 Gene dauerless Regulates Dauer Development and Intraspecific Competition in Nematodes
592 by Copy Number Variation. PLOS Genetics. 2015;11(6). doi: 10.1371/journal.pgen.1005146.
593 22. Li D, Yan Z, Lu L, Jiang H, Wang W. Pleiotropy of the de novo-originated gene
594 MDF1. Scientific Reports. 2014;4(1). doi: 10.1038/srep07280.
595 23. Neme R, Tautz D. Fast turnover of genome transcription across evolutionary time
596 exposes entire non-coding DNA to de novo gene emergence. eLife. 2016;5. doi:
597 10.7554/eLife.09977.
598 24. Kapranov P, Willingham AT, Gingeras TR. Genome-wide transcription and the
599 implications for genomic organization. Nat Rev Genet. 2007;8(6):413-23. doi:
600 10.1038/nrg2083.
601 25. Ruiz-Orera J, Verdaguer-Grau P, Villanueva-Canas JL, Messeguer X, Alba MM.
602 Translation of neutrally evolving peptides provides a basis for de novo gene evolution. Nat
603 Ecol Evol. 2018;2(5):890-6. Epub 2018/03/21. doi: 10.1038/s41559-018-0506-6. PubMed
604 PMID: 29556078.
605 26. Ingolia Nicholas T, Brar Gloria A, Stern-Ginossar N, Harris Michael S, Talhouarne
606 Gaëlle JS, Jackson Sarah E, et al. Ribosome Profiling Reveals Pervasive Translation Outside
607 of Annotated Protein-Coding Genes. Cell Reports. 2014;8(5):1365-79. doi:
608 10.1016/j.celrep.2014.07.045.
609 27. Prabh N, Rödelsperger C. Are orphan genes protein-coding, prediction artifacts, or
610 non-coding RNAs? BMC Bioinformatics. 2016;17(1). doi: 10.1186/s12859-016-1102-x.
611 28. Zhang L, Ren Y, Yang T, Li G, Chen J, Gschwend AR, et al. Rapid evolution of
612 protein diversity by de novo origination in Oryza. Nature Ecology & Evolution.
613 2019;3(4):679-90. doi: 10.1038/s41559-019-0822-5.
614 29. Schmitz JF, Ullrich KK, Bornberg-Bauer E. Incipient de novo genes can evolve from
615 frozen accidents that escaped rapid transcript turnover. Nat Ecol Evol. 2018;2(10):1626-32.
616 Epub 2018/09/12. doi: 10.1038/s41559-018-0639-7. PubMed PMID: 30201962.
617 30. Ruiz-Orera J, Alba MM. Translation of Small Open Reading Frames: Roles in
618 Regulation and Evolutionary Innovation. Trends Genet. 2019;35(3):186-98. Epub
619 2019/01/05. doi: 10.1016/j.tig.2018.12.003. PubMed PMID: 30606460.
620 31. Tautz D, Domazet-Loso T. The evolutionary origin of orphan genes. Nat Rev Genet.
621 2011;12(10):692-702. Epub 2011/09/01. doi: 10.1038/nrg3053. PubMed PMID: 21878963.
622 32. Wu X, Sharp Phillip A. Divergent Transcription: A Driving Force for New Gene
623 Origination? Cell. 2013;155(5):990-6. doi: 10.1016/j.cell.2013.10.048.

624 33. Levine M, Cattoglio C, Tjian R. Looping back to leap forward: transcription enters a
625 new era. Cell. 2014;157(1):13-25. Epub 2014/04/01. doi: 10.1016/j.cell.2014.02.009.
626 PubMed PMID: 24679523; PubMed Central PMCID: PMCPMC4059561.
627 34. Kim T-K, Hemberg M, Gray JM, Costa AM, Bear DM, Wu J, et al. Widespread
628 transcription at neuronal activity-regulated enhancers. Nature. 2010;465(7295):182-7. doi:
629 10.1038/nature09033.
630 35. Evdokimova V, Ruzanov P, Imataka H, Raught B, Svitkin Y, Ovchinnikov LP, et al.
631 The major mRNA-associated protein YB-1 is a potent 5' cap-dependent mRNA stabilizer.
632 EMBO J. 2001;20(19):5491-502. Epub 2001/09/28. doi: 10.1093/emboj/20.19.5491. PubMed
633 PMID: 11574481; PubMed Central PMCID: PMCPMC125650.
634 36. Shatkin A. Capping of eucaryotic mRNAs. Cell. 1976;9(4):645-53. doi:
635 10.1016/0092-8674(76)90128-8.
636 37. Visa N, Izaurralde E, Ferreira J, Daneholt B, Mattaj IW. A nuclear cap-binding
637 complex binds Balbiani ring pre-mRNA cotranscriptionally and accompanies the
638 ribonucleoprotein particle during nuclear export. J Cell Biol. 1996;133(1):5-14. Epub
639 1996/04/01. PubMed PMID: 8601613; PubMed Central PMCID: PMCPMC2120770.
640 38. Heintzman ND, Stuart RK, Hon G, Fu Y, Ching CW, Hawkins RD, et al. Distinct and
641 predictive chromatin signatures of transcriptional promoters and enhancers in the human
642 genome. Nat Genet. 2007;39(3):311-8. Epub 2007/02/06. doi: 10.1038/ng1966. PubMed
643 PMID: 17277777.
644 39. An integrated encyclopedia of DNA elements in the human genome. Nature.
645 2012;489(7414):57-74. doi: 10.1038/nature11247.
646 40. Creyghton MP, Cheng AW, Welstead GG, Kooistra T, Carey BW, Steine EJ, et al.
647 Histone H3K27ac separates active from poised enhancers and predicts developmental state.
648 Proceedings of the National Academy of Sciences. 2010;107(50):21931-6. doi:
649 10.1073/pnas.1016071107.
650 41. Berthelot C, Villar D, Horvath JE, Odom DT, Flicek P. Complexity and conservation
651 of regulatory landscapes underlie evolutionary resilience of mammalian gene expression. Nat
652 Ecol Evol. 2018;2(1):152-63. Epub 2017/11/29. doi: 10.1038/s41559-017-0377-2. PubMed
653 PMID: 29180706; PubMed Central PMCID: PMCPMC5733139.
654 42. Andersson R, Gebhard C, Miguel-Escalada I, Hoof I, Bornholdt J, Boyd M, et al. An
655 atlas of active enhancers across human cell types and tissues. Nature. 2014;507(7493):455-
656 61. doi: 10.1038/nature12787.
657 43. Carelli FN, Liechti A, Halbert J, Warnefors M, Kaessmann H. Repurposing of
658 promoters and enhancers during mammalian evolution. Nat Commun. 2018;9(1):4066. Epub
659 2018/10/06. doi: 10.1038/s41467-018-06544-z. PubMed PMID: 30287902; PubMed Central
660 PMCID: PMCPMC6172195.
661 44. Ong C-T, Corces VG. CTCF: an architectural protein bridging genome topology and
662 function. Nat Rev Genet. 2014;15(4):234-46. doi: 10.1038/nrg3663.
663 45. Cusanovich DA, Hill AJ, Aghamirzaie D, Daza RM, Pliner HA, Berletch JB, et al. A
664 Single-Cell Atlas of In Vivo Mammalian Chromatin Accessibility. Cell. 2018;174(5):1309-
665 24 e18. Epub 2018/08/07. doi: 10.1016/j.cell.2018.06.052. PubMed PMID: 30078704;
666 PubMed Central PMCID: PMCPMC6158300.
667 46. Neme R, Tautz D. Phylogenetic patterns of emergence of new genes support a model
668 of frequent de novo evolution. BMC Genomics. 2013;14(1). doi: 10.1186/1471-2164-14-117.
669 47. Tabula Muris C, Overall c, Logistical c, Organ c, processing, Library p, et al. Single-
670 cell transcriptomics of 20 mouse organs creates a Tabula Muris. Nature.
671 2018;562(7727):367-72. Epub 2018/10/05. doi: 10.1038/s41586-018-0590-4. PubMed
672 PMID: 30283141.

673 48. Kryuchkova-Mostacci N, Robinson-Rechavi M. Tissue-Specific Evolution of Protein
674 Coding Genes in Human and Mouse. PLoS One. 2015;10(6):e0131673. Epub 2015/06/30.
675 doi: 10.1371/journal.pone.0131673. PubMed PMID: 26121354; PubMed Central PMCID:
676 PMCPMC4488272.
677 49. Mantsoki A, Devailly G, Joshi A. Gene expression variability in mammalian
678 embryonic stem cells using single cell RNA-seq data. Computational Biology and Chemistry.
679 2016;63:52-61. doi: 10.1016/j.compbiolchem.2016.02.004.
680 50. Werner MS, Sieriebriennikov B, Prabh N, Loschko T, Lanz C, Sommer RJ. Young
681 genes have distinct gene structure, epigenetic profiles, and transcriptional regulation. Genome
682 Research. 2018;28(11):1675-87. doi: 10.1101/gr.234872.118.
683 51. Sebe-Pedros A, Saudemont B, Chomsky E, Plessier F, Mailhe MP, Renno J, et al.
684 Cnidarian Cell Type Diversity and Regulation Revealed by Whole-Organism Single-Cell
685 RNA-Seq. Cell. 2018;173(6):1520-34 e20. Epub 2018/06/02. doi: 10.1016/j.cell.2018.05.019.
686 PubMed PMID: 29856957.
687 52. Schwaiger M, Schonauer A, Rendeiro AF, Pribitzer C, Schauer A, Gilles AF, et al.
688 Evolutionary conservation of the eumetazoan gene regulatory landscape. Genome Research.
689 2014;24(4):639-50. doi: 10.1101/gr.162529.113.
690 53. Kvon EZ, Kazmar T, Stampfel G, Yáñez-Cuna JO, Pagani M, Schernhuber K, et al.
691 Genome-scale functional characterization of Drosophila developmental enhancers in vivo.
692 Nature. 2014;512(7512):91-5. doi: 10.1038/nature13395.
693 54. Capra JA, Pollard KS, Singh M. Novel genes exhibit distinct patterns of function
694 acquisition and network integration. Genome Biol. 2010;11(12):R127. Epub 2010/12/29. doi:
695 10.1186/gb-2010-11-12-r127. PubMed PMID: 21187012; PubMed Central PMCID:
696 PMCPMC3046487.
697 55. Abrusán G. Integration of New Genes into Cellular Networks, and Their Structural
698 Maturation. Genetics. 2013;195(4):1407-17. doi: 10.1534/genetics.113.152256.
699 56. Warnefors M, Eyre-Walker A. The Accumulation of Gene Regulation Through Time.
700 Genome Biology and Evolution. 2011;3:667-73. doi: 10.1093/gbe/evr019.
701 57. Carroll SB. Chance and necessity: the evolution of morphological complexity and
702 diversity. Nature. 2001;409(6823):1102-9. Epub 2001/03/10. doi: 10.1038/35059227.
703 PubMed PMID: 11234024.
704 58. Domazet-Lošo T, Brajković J, Tautz D. A phylostratigraphy approach to uncover the
705 genomic history of major adaptations in metazoan lineages. Trends in Genetics.
706 2007;23(11):533-9. doi: 10.1016/j.tig.2007.08.014.
707 59. Buenrostro JD, Giresi PG, Zaba LC, Chang HY, Greenleaf WJ. Transposition of
708 native chromatin for fast and sensitive epigenomic profiling of open chromatin, DNA-
709 binding proteins and nucleosome position. Nature Methods. 2013;10(12):1213-8. doi:
710 10.1038/nmeth.2688.
711 60. Kent WJ, Sugnet CW, Furey TS, Roskin KM, Pringle TH, Zahler AM, et al. The
712 Human Genome Browser at UCSC. Genome Research. 2002;12(6):996-1006. doi:
713 10.1101/gr.229102.
714 61. Quinlan AR, Hall IM. BEDTools: a flexible suite of utilities for comparing genomic
715 features. Bioinformatics. 2010;26(6):841-2. doi: 10.1093/bioinformatics/btq033.
716 62. Lizio M, Harshbarger J, Shimoji H, Severin J, Kasukawa T, Sahin S, et al. Gateways
717 to the FANTOM5 promoter level mammalian expression atlas. Genome Biology. 2015;16(1).
718 doi: 10.1186/s13059-014-0560-6.
719 63. Noguchi S, Arakawa T, Fukuda S, Furuno M, Hasegawa A, Hori F, et al. FANTOM5
720 CAGE profiles of human and mouse samples. Scientific Data. 2017;4. doi:
721 10.1038/sdata.2017.112.

64. Shiraki T, Kondo S, Katayama S, Waki K, Kasukawa T, Kawaji H, et al. Cap analysis gene expression for high-throughput analysis of transcriptional starting point and identification of promoter usage. Proceedings of the National Academy of Sciences. 2003;100(26):15776-81. doi: 10.1073/pnas.2136655100.

65. Ingolia NT. Ribosome profiling: new views of translation, from single codons to genome scale. Nat Rev Genet. 2014;15(3):205-13. doi: 10.1038/nrg3645.

66. Michel AM, Fox G, M. Kiran A, De Bo C, O'Connor PBF, Heaphy SM, et al. GWIPS-viz: development of a ribo-seq genome browser. Nucleic Acids Research. 2014;42(D1):D859-D64. doi: 10.1093/nar/gkt1035.

67. Dalby M, Rennie, Sarah, & Andersson, Robin. FANTOM5 transcribed enhancers in mm10 Zenodo2018.

68. Pliner HA, Packer JS, McFaline-Figueroa JL, Cusanovich DA, Daza RM, Aghamirzaie D, et al. Cicero Predicts cis-Regulatory DNA Interactions from Single-Cell Chromatin Accessibility Data. Molecular Cell. 2018;71(5):858-71.e8. doi: 10.1016/j.molcel.2018.06.044.

69. Cunningham F, Achuthan P, Akanni W, Allen J, Amode MR, Armean IM, et al. Ensembl 2019. Nucleic Acids Res. 2019;47(D1):D745-D51. Epub 2018/11/09. doi: 10.1093/nar/gky1113. PubMed PMID: 30407521; PubMed Central PMCID: PMCPMC6323964.